



OPEN ACCESS

EDITED BY

Masaki Ueno,
Niigata University, Japan

REVIEWED BY

Edmund R. Hollis,
Burke Neurological Institute (BNI),
United States
Tatsuya Umeda,
Kyoto University, Japan

*CORRESPONDENCE

D. J. Guggenmos
✉ dguggenmos@kumc.edu

RECEIVED 25 January 2023

ACCEPTED 24 April 2023

PUBLISHED 02 June 2023

CITATION

Hayley P, Tucek C, Dalla S, Borrell J,
Murphy MD, Nudo RJ and
Guggenmos DJ (2023) Post-ischemic
reorganization of sensory responses in cerebral
cortex.
Front. Neurosci. 17:1151309.
doi: 10.3389/fnins.2023.1151309

COPYRIGHT

© 2023 Hayley, Tucek, Dalla, Borrell, Murphy,
Nudo and Guggenmos. This is an open-access
article distributed under the terms of the
[Creative Commons Attribution License \(CC BY\)](https://creativecommons.org/licenses/by/4.0/).
The use, distribution or reproduction in other
forums is permitted, provided the original
author(s) and the copyright owner(s) are
credited and that the original publication in this
journal is cited, in accordance with accepted
academic practice. No use, distribution or
reproduction is permitted which does not
comply with these terms.

Post-ischemic reorganization of sensory responses in cerebral cortex

P. Hayley¹, C. Tucek², S. Dalla³, J. Borrell⁴, M. D. Murphy⁴,
R. J. Nudo⁵ and D. J. Guggenmos^{5*}

¹Department of Molecular and Integrative Physiology, University of Kansas Medical Center, Kansas City, KS, United States, ²Department of Neurosurgery, University of Kansas Medical Center, Kansas City, KS, United States, ³University of Kansas, School of Medicine Wichita, Kansas City, KS, United States, ⁴Bioengineering Program, University of Kansas, Lawrence, KS, United States, ⁵Department of Rehabilitation Medicine and the Landon Center on Aging, University of Kansas Medical Center, Kansas City, KS, United States

Introduction: Sensorimotor integration is critical for generating skilled, volitional movements. While stroke tends to impact motor function, there are also often associated sensory deficits that contribute to overall behavioral deficits. Because many of the cortico-cortical projections participating in the generation of volitional movement either target or pass-through primary motor cortex (in rats, caudal forelimb area; CFA), any damage to CFA can lead to a subsequent disruption in information flow. As a result, the loss of sensory feedback is thought to contribute to motor dysfunction even when sensory areas are spared from injury. Previous research has suggested that the restoration of sensorimotor integration through reorganization or *de novo* neuronal connections is important for restoring function. Our goal was to determine if there was crosstalk between sensorimotor cortical areas with recovery from a primary motor cortex injury. First, we investigated if peripheral sensory stimulation would evoke responses in the rostral forelimb area (RFA), a rodent homologue to premotor cortex. We then sought to identify whether intracortical microstimulation-evoked activity in RFA would reciprocally modify the sensory response.

Methods: We used seven rats with an ischemic lesion of CFA. Four weeks after injury, the rats' forepaw was mechanically stimulated under anesthesia and neural activity was recorded in the cortex. In a subset of trials, a small intracortical stimulation pulse was delivered in RFA either individually or paired with peripheral sensory stimulation.

Results: Our results point to post-ischemic connectivity between premotor and sensory cortex that may be related to functional recovery. Premotor recruitment during the sensory response was seen with a peak in spiking within RFA after the peripheral solenoid stimulation despite the damage to CFA. Furthermore, stimulation in RFA modulated and disrupted the sensory response in sensory cortex.

Discussion: The presence of a sensory response in RFA and the sensitivity of S1 to modulation by intracortical stimulation provides additional evidence for functional connectivity between premotor and somatosensory cortex. The strength of the modulatory effect may be related to the extent of the injury and the subsequent reshaping of cortical connections in response to network disruption.

KEYWORDS

plasticity, somatosensory, stimulation, activity, cerebral cortex

1. Introduction

The integration of sensory information within the motor cortex is an important feature of adaptive motor control. Sanes et al. (1992) showed forelimb position modified motor cortex somatotopy, underlining the influence of sensory feedback on motor output. It is theorized that sensory prediction encodes an internal model necessary for generating task-specific forces which are then fine-tuned via prediction error when there is a mismatch between the projected trajectory and the resulting action (Shadmehr et al., 2010). While the cerebellum is generally thought of as the primary driver of error correction using ascending sensory information, recent evidence suggests that the somatosensory cortex also makes a significant contribution to this process (Thoroughman and Shadmehr, 2000; Tseng et al., 2007). Photoinhibition of somatosensory cortex during a reach behavior limited adaptation to task perturbation, along with similar results from human somatosensory cortex inhibition during motor learning, add credence to the presence of sensorimotor interactions within the cerebral cortex that allow for adaptive motor behavior (Vidoni et al., 2010; Mathis et al., 2017). Therefore, the reciprocal communication between somatosensory and motor cortex is likely an important part of the generation of complex volitional movements.

Disruption of sensorimotor connectivity, as occurs in acquired brain injury, often leads to a more severe motor impairment than what might be predicted based on damage to motor structures alone since there is an additional loss of sensory integration. In line with this, Shadmehr and Krakauer (2008) propose that the deficits that arise with corticospinal tract injury are more than a downstream failure to transmit a control signal that may be expected with loss of corticospinal neurons. In their review, they draw parallels between subcortical stroke cases to patients with sensory dysfunction as they both display an inability to construct an accurate internal model for the movement. The loss of behavioral stability across trials in patients with motor impairments after stroke further supports the absence of integrated sensory predictions (Kim et al., 2016). The basis for sensory dysfunction in motor impairment can be examined in greater detail in animal models with a focal cortical lesion (Nudo et al., 2000). Injury to motor cortex likely disrupts a wide array of neural connections, including those from sensory cortex (Friel et al., 2005). The damage could directly affect axonal projections or indirectly cause the loss of input; in either case, the injury results in the loss of shared information between cortical areas (Contestabile et al., 2018; Lee et al., 2020). Even with some recovery via spared motor areas like premotor cortex and its descending motor projections, the loss of sensory input may still restrict full behavioral recovery. However, there is often novel, large-scale structural reorganization during spontaneous recovery to compensate for these losses and support the restitution of sensorimotor integration (Carmichael and Chesselet, 2002; Dancause et al., 2005; Frías et al., 2018). Thus, the post-injury plasticity of cortex is a potential substrate for re-establishing the sensory feedback that is necessary for motor strategies used in activities of daily living (Harrison et al., 2013).

Somatosensory evoked potentials during motor learning are sensitive to task adaptation, leading us to consider the ways somatosensory responses within the cortex could be used as an index of sensorimotor function (Nasir et al., 2013). The somatosensory system codes information for both latency and magnitude of the

response which are likely altered after injury as a part of ongoing plastic processes (Tutunculer et al., 2006; Moxon et al., 2008; Padberg et al., 2010; Sweetnam and Brown, 2013). The goal of this study was to uncover mutual communication between premotor and somatosensory cortex following recovery from a primary motor cortex lesion by measuring sensory related activity within the spared premotor cortex and modulation of sensory responses in somatosensory cortex by premotor activity. Rats have a single putative premotor area known as the rostral forelimb area (RFA). While the majority of sensorimotor connectivity is mediated by the primary motor cortex (caudal forelimb area; CFA), direct, reciprocal corticocortical projections between RFA and somatosensory cortex (S1) also exist (Rouiller et al., 1993). The anatomical connections and single premotor cortical area make rats a prime model for sensorimotor assays. If disruption of CFA and S1 connectivity through injury results in a subsequent restoration of sensorimotor integration through extant and *de novo* connections between RFA and S1, we expect that there will be modulation of cortical processing of the somatosensory response to peripheral stimulation.

To study this, rats were given a focal ischemic lesion within CFA. Four weeks later, the rats underwent a terminal procedure in which the neural responses to mechanical stimulation of the forepaw were recorded within the somatosensory and premotor cortex and modulated by intracortical microstimulation (ICMS) delivery. We found there are clear responses to peripheral somatosensory stimulation in both RFA and S1 after lesioning CFA that, while distinct, have a shared peak in spiking activity 50 ms after onset. This stands in contrast to previous work which resulted in the abolishment of a somatosensory response in premotor cortex without mediation of the primary motor cortex, reinforcing the idea that there is direct recruitment of premotor cortex with somatosensory processing during recovery (Kunori and Takashima, 2016). Of note, rats with larger lesion volumes displayed a significant relationship for increased spiking during this later sensory response with a concurrent reduction in the early peak specific to S1 which could be a result of increasing sensorimotor integration between the cortical areas. The addition of a stimulus in RFA clearly disrupted patterns in the somatosensory response in RFA and S1 and predicted an increase in the weight of the shared response regardless of area. The modulation of the somatosensory response by ICMS in S1 along with RFA supports the establishment of their intercommunication in recovery. Together, these results provide evidence for a relationship between premotor and somatosensory cortex in sensory processing after primary motor cortex injury.

2. Materials and methods

2.1. Animals

A total of seven young-adult male Long-Evans rats (325 g–335 g; 10 weeks on arrival; Charles River) were included in this study after meeting inclusion criteria on the behavioral task and surviving both surgical procedures (out of 12 animals). All procedures were approved by the University of Kansas Medical Center Institutional Animal Care and Use Committee and complied with the *Guide for the Care and Use of Laboratory Animals (Eighth Edition, The National Academies Press, 2010)*.

2.2. Training procedures

Rats were initially trained to retrieve pellets from a semi-automated behavioral box (adapted from the box described by Bundy et al., 2019). The task requires the rats to reach out of a slot in a Plexiglas behavioral box to retrieve a food pellet (45-mg Dustless Precision Rodent Pellets; Bio-Serv). The box is designed with a door which closes after each reach attempt through an infrared beam break, constituting a single trial. The trial was deemed successful if the rat grasped the pellet and brought it into the box without dropping it. Multiple initiations of reaches within a single trial were noted but were only scored as successful if the retrieval was complete. The percentage of successful retrievals over all trials within a single session, which lasted for approximately an hour, was measured as an indicator of behavioral ability. Rats who reached 60 reaches within the first 15 min were stopped and the sessions were considered complete. Behavioral training took approximately 2 weeks, by which point rats were required to successfully retrieve pellets with a 60% success rate at least once prior to continuation in the study. One of the original goals of these studies was to examine the effects of post-injury experience on sensorimotor integration. However, the differences between animals with rehabilitative training and those without were minimal compared to the variability in lesion size and corresponding functional impairments across groups, so the groups were collapsed for analysis (Supplementary Figure 1, Table 1).

2.3. Initial surgery and injury

Rats were anesthetized using an initial dose of isoflurane followed by bolus injections of ketamine i.p. and xylazine i.m. The animal's anesthetic state was monitored and maintained using 0.1 cc intramuscular injections of ketamine (100 mg/ml), supplemented by xylazine (20 mg/ml) or isoflurane as appropriate. Six burr holes were made using a dental burr bit at 1.5, 0.5, -0.5 mm anterior/posterior and 2.5 and 3.5 mm lateral to bregma in order to target the caudal forelimb area (CFA) contralateral to the preferred reaching forelimb (Nishibe et al., 2015). Three boluses of 110 nl of the vasoconstrictor endothelin-1 (ET-1) were delivered at each site for a total of 990 nl to create a focal ischemic lesion. Rats were administered buprenorphine and acetaminophen over the course of 48-h following the injury procedure. In general, rats recovered well from the ischemic lesion surgeries.

2.4. Secondary surgery and data collection

On post-operative day 26, all rats underwent a terminal procedure to test the ability to evoke and modulate the response to peripheral sensory stimulation in the forelimb somatosensory cortex (S1) and rostral forelimb area (RFA). After anesthetization and fixation in the stereotaxic frame, the incision was re-opened and a laminectomy was made at the base of the skull to allow drainage of cerebrospinal fluid and prevent edema. Two craniectomies were performed using a dental burr bit to expose the sensorimotor cortex of both hemispheres. RFA was identified by using stereotaxic coordinates to find an approximate location, evoking motor movements using a standard intracortical microstimulation (ICMS) mapping procedure, and roughly

identifying map borders. (Nishibe et al., 2010) Additional 0.1 cc boluses of ketamine (100 mg/ml) were administered as necessary in between experimental blocks to maintain the anesthetic plane. Occasionally, isoflurane (0.5–1.5%) was administered for brief, 20–30 s periods to reduce spontaneous whisking that introduced significant artifact in the electrophysiologic recordings. Recordings were not performed during or immediately after this application. Using pulled glass micropipettes (3.5 M NaCl; platinum wire) with tapered tip diameters between 10 and 25- μ m, motor areas were identified by lowering the microelectrode to a depth of 1,500- μ m using a microdrive (Narishige), delivering cathodal bursts of 13 stimulus pulses (1-Hz trains at 350-Hz), through a constant current stimulator (BAK) and ramping up current, up to 60 microamps, and observing any evoked movements. ICMS trains were coupled to an audio amplifier, enabling experimenters to associate joint movements with each train burst. The receptive fields of S1 were localized by inserting a microelectrode array (MEA; NeuroNexus A4 \times 8-5 mm-100-400-703) into the target area connected to a digitizing headstage and acquisition hardware (Intan Technologies). The forelimb area of S1 was defined by the ability to evoke output by manually palpating the contralateral paw while listening for audible spiking responses on different sites within the array. The first insertion site with any responsive channels was used to avoid exacerbating edema with multiple insertions of the MEA. A more detailed topography of forelimb somatosensory cortex was then resolved by switching to Von Frey microfilaments. Following identification of S1 and RFA, two MEAs were lowered into these areas using micropositioners. Response properties of neural units were recorded from 4-shank (shank-spacing of 400- μ m) polymeric MEAs with 8 electrodes (site-area of 703- μ m²) per shank (site-spacing of 100- μ m; NeuroNexus A4 \times 8-5 mm-100-400-703) with a sampling frequency of 30-kHz (Intan Stimulation/Recording Controller). The median impedance of the MEAs was 529.6 \pm 168.8 kOhms. Additional application of isoflurane was critical to ensure that large deflections in the local field potential that appeared to be related to whisking were mitigated and did not contaminate the recorded response to sensory stimulation. Stimulation was delivered using two modalities: electrical microstimulation delivered in the premotor cortex and mechanical sensory stimulation of the forelimb using a solenoid. Three types of trials were cycled through during the neural recordings: solenoid-only peripheral stimulation ("Solenoid"), intracortical microstimulation-only ("ICMS"), or both types of stimulation at a set latency for each experiment ("ICMS + Solenoid"). A miniature 5 V solenoid (ID 2776; Adafruit) was clamped to the stereotaxic apparatus and positioned next to the forelimb to contact a site which strongly elicited an increase in spiking on the MEA in S1. The solenoid was placed at a distance where the small pin contacted the forepaw during its range of movement and displaced it with a load less than 80 g. The solenoid was activated in 1-Hz intervals. While the solenoid is not as sensitive as force-controlled mechanisms like that described by Emanuel et al. (2021), it is similar to the setup described in Foffani et al. (2004) and Moxon et al. (2008). For the ICMS trials, a single cathodal-leading, bi-phasic square wave stimulation pulse of 60 μ A and with a phase duration of 100- μ sec per phase, insufficient for evoking motor movements, was delivered using a single electrode site from within the recording array in RFA. A digital signal generator (Master-9; A.M.P.I.) was used to cycle through logical combinations of digital inputs to the combined recording and stimulation unit so that each experiment cycled serially through 100 trials each of the three types of trials for a

single experimental block. A stimulation-state machine module embedded in the FPGA of the recording and stimulation unit was used to implement any delay between solenoid and ICMS, or between ICMS and the onset of the trial indicator (Figure 1).

2.5. Histological preparation

Immediately following the terminal procedure, the rats were injected with pentobarbital (Beuthanasia-D) and transcardially perfused with 0.1 M saline solution with heparin and lidocaine followed by 4% paraformaldehyde. The brains were extracted, gelatin embedded, and sectioned coronally at a thickness of 50- μ m using a freezing, sliding microtome. The sections were mounted on slides and stained with cresyl violet. An example of coronal hemisections corresponding to CFA are shown in Figure 2. Sections were analyzed under a light microscope (Zeiss AxioImager M2) and sampled at 0.6-mm intervals. Hemispheric volume through the sensorimotor

cortex was estimated using the Cavalieri method, labeling the region of interest, which was drawn around gaps and non-viable tissue in the injured cortex to outline the lesion area, with markers (Figure 2B). The stereotaxic coordinates of a sample section for each rat was identified by comparing to anatomical landmarks from Paxinos and Watson (2006) and used to roughly align the reconstructed lesions on a representative diagram of a rat brain (Supplementary Figure 2).

2.6. Neural data processing

2.6.1. Spike detection

Unit activity was filtered using a 4th-order elliptic IIR filter with passband cutoffs of 300-Hz and 5,000-Hz. After bandpass filtering, a virtual common reference was estimated as the ensemble mean of all channels on a given MEA, which was then subtracted from each individual channel signal. After filtering, spikes were detected using a smoothed nonlinear energy operator (SNEO; Mukhopadhyay and

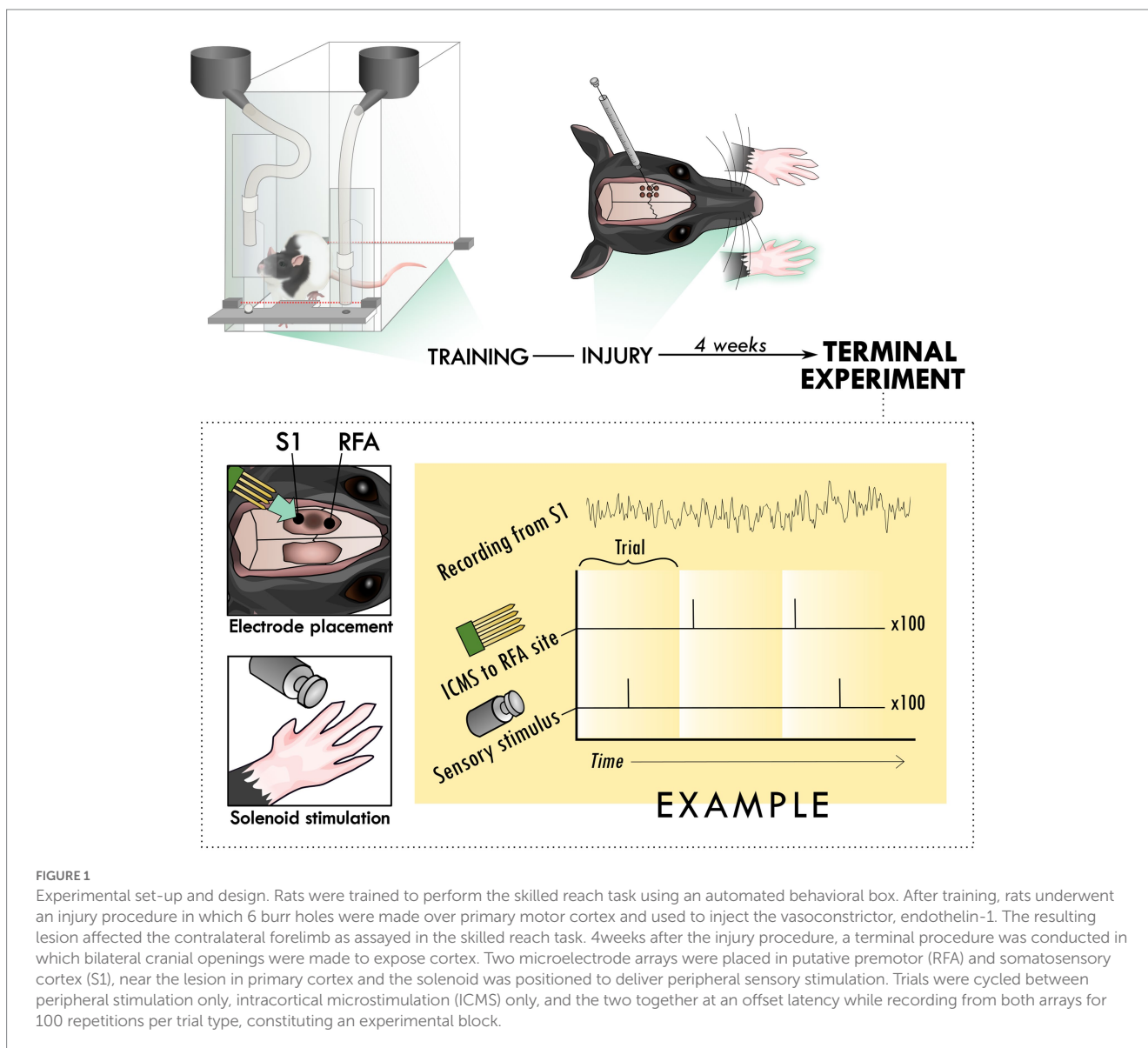
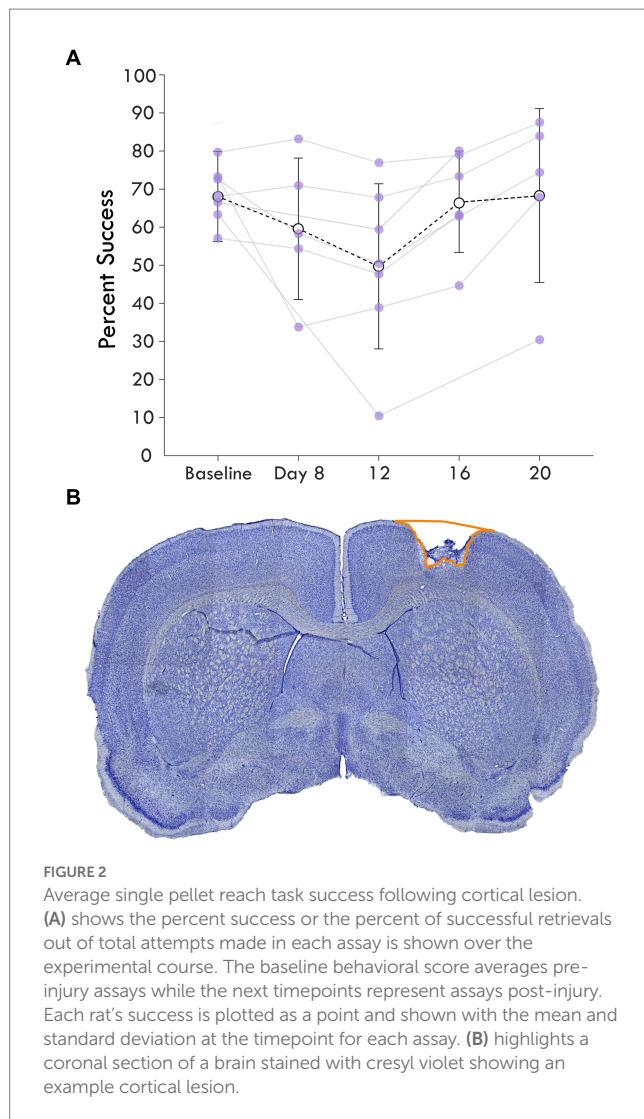


FIGURE 1

Experimental set-up and design. Rats were trained to perform the skilled reach task using an automated behavioral box. After training, rats underwent an injury procedure in which 6 burr holes were made over primary motor cortex and used to inject the vasoconstrictor, endothelin-1. The resulting lesion affected the contralateral forelimb as assayed in the skilled reach task. 4 weeks after the injury procedure, a terminal procedure was conducted in which bilateral cranial openings were made to expose cortex. Two microelectrode arrays were placed in putative premotor (RFA) and somatosensory cortex (S1), near the lesion in primary cortex and the solenoid was positioned to deliver peripheral sensory stimulation. Trials were cycled between peripheral stimulation only, intracortical microstimulation (ICMS) only, and the two together at an offset latency while recording from both arrays for 100 repetitions per trial type, constituting an experimental block.



Ray, 1998), with a smoothing width of five samples and a minimum amplitude threshold of $15\text{-}\mu\text{V}$. This detection method captured the physiological response of multi-unit activity in a manner that was consistent with previously reported results (Averna et al., 2021; Carè et al., 2022), indicating its acceptability as a proxy for neural excitation and inhibition in response to the peripheral sensory stimulus. For all trials, any absolute deviation greater than $450\mu\text{V}$ was considered artifact and spikes 4 ms before or after the artifact were discarded. Because the stimulation produced such an artifact, there was an imposed blanking period around the ICMS pulse.

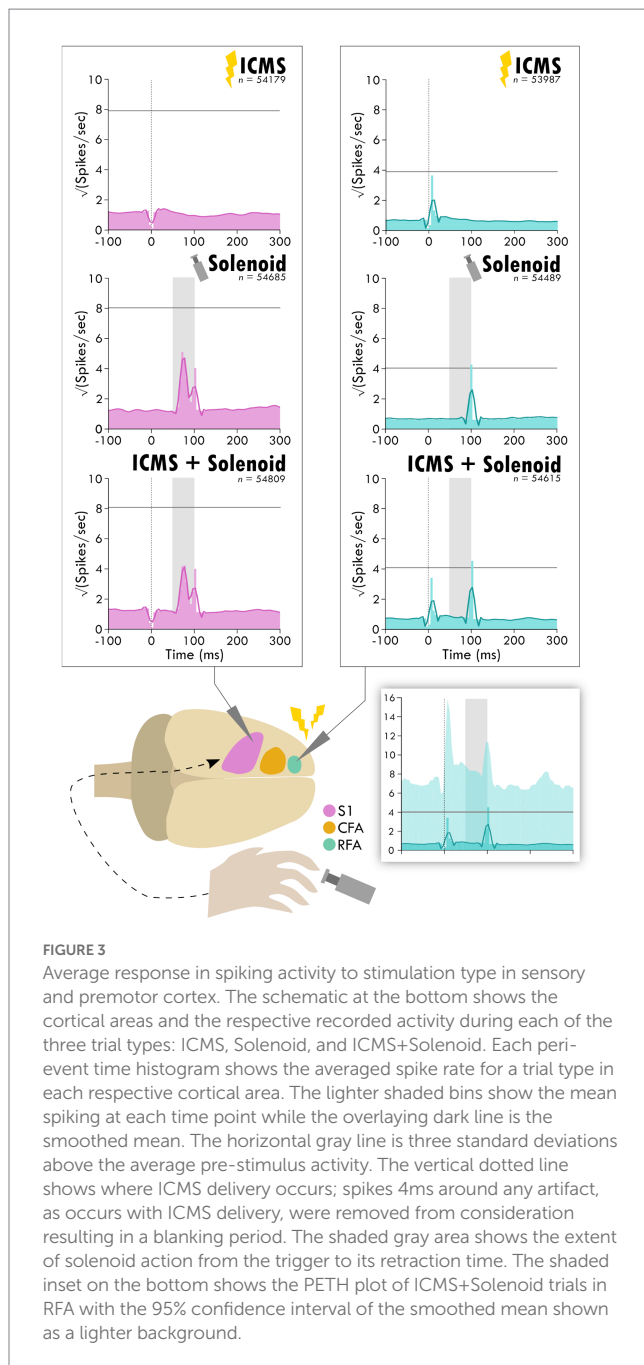
2.6.2. Spike unit analysis

The spike rate was determined by taking the square root of the mean multi-unit spike counts in 5 ms bins on a per-channel basis for each experimental block. The spike rate was then smoothed using a Savitzky–Golay filter. Mean baseline spike rates were computed on a per-channel basis for each experimental block, averaging together bins prior to the beginning of the trial (labeled the zero time-point in figures). Bins at the beginning and end of the baseline period corresponding to 50 ms were disregarded in order to avoid artifact introduced by the filtering step, resulting in a

150 ms window. The mean and standard deviation of the baseline spike rates were then used to determine a threshold for significant evoked activity (three times the standard deviation). Channels from a given trial with a baseline spike rate below $2.4\sqrt{\text{spikes/s}}$ ($<1\%$ of all data collected) were removed from consideration because the low event rate would be insufficient to power statistical analyses. For each peri-event time histogram, the square-root-transformed average spike rates were computed in the same way for each grouped experimental variable (i.e., trial type and area) and plotted for each bin. A Savitzky–Golay filter was applied to smooth the spike rates to find the corresponding 95% confidence band at each time point. Smoothing used a 21-sample Kaiser window with shape parameter set to 38 to fit a 3rd order polynomial to the sequence of spike times.

2.7. Component analysis

The average spike rates of channels for each experimental block during the 250-ms immediately following the solenoid onset were analyzed by trial type to determine their top-3 principal components, collapsing both animal and area in the process. Ideally, a single linear basis decomposition could be applied to the stimulus-conditioned mean evoked spike rates observed from all included channels, such that trajectories resembling stereotyped stimulus-evoked responses comprise a primary basis subspace, enabling statistical comparison of these responses and avoiding issues of multiple comparisons in response criteria. However, projections of the ICMS-only trials during the considered time-period along this basis would lack the solenoid-evoked response and be unhelpful in accurately reconstructing the original observations. Therefore, we used a combination approach where we derived components for all three trial types to best describe the response of each and then a combined set of components for the Solenoid and ICMS + Solenoid trials for better comparison of the solenoid response. We first applied principal components analysis (PCA; MATLAB R2017a+ 'pca' function with 'Algorithm' parameter set to 'svd') to qualitatively describe the different types of evoked responses for each condition, applying a singular value decomposition to the mean channel spike rates separately for each stimulus type; then, using the groupings for which the same basis subspace could accurately reconstruct the original observations, we seeded a reconstructed-independent components analysis algorithm (r-ICA; MATLAB R2017a+ 'rica' function from the Statistics and Machine Learning Toolbox) using the top-3 combined-basis eigenvectors to recover a basis for the sets of components described above (Supplementary Figure 6). Detailed parameterization is included with all code used in analyses, which is available at <https://github.com/Cortical-Plasticity-Lab/Solenoid-Ephys-Analyses>. Details of the MATLAB r-ICA implementation are summarized here for reproducibility: The r-ICA algorithm maps input data to output features by minimizing a standard limited memory Broyden-Fletcher-Goldfarb-Shanno (LBFGS) quasi-Newton optimizer. In this case, we let each observation x be the set of each mean spike rates for a given channel; we would like to recover both s and A such that each column of s is statistically independent from the other while still allowing us to accurately reconstruct each x in the observed data:



$$x = \mu + As$$

- x is a column vector of length p .
- μ is a column vector of length p representing a constant term.
- s is a column vector of length q whose elements are zero mean, unit variance random variables that are statistically independent of each other.
- A is a mixing matrix of size p -by- q .

To provide a way to fit this regression, we require that the initial weights for A are set to the top- k principal components for X , the set of all mean spike rates (such that rows of X are time samples and each

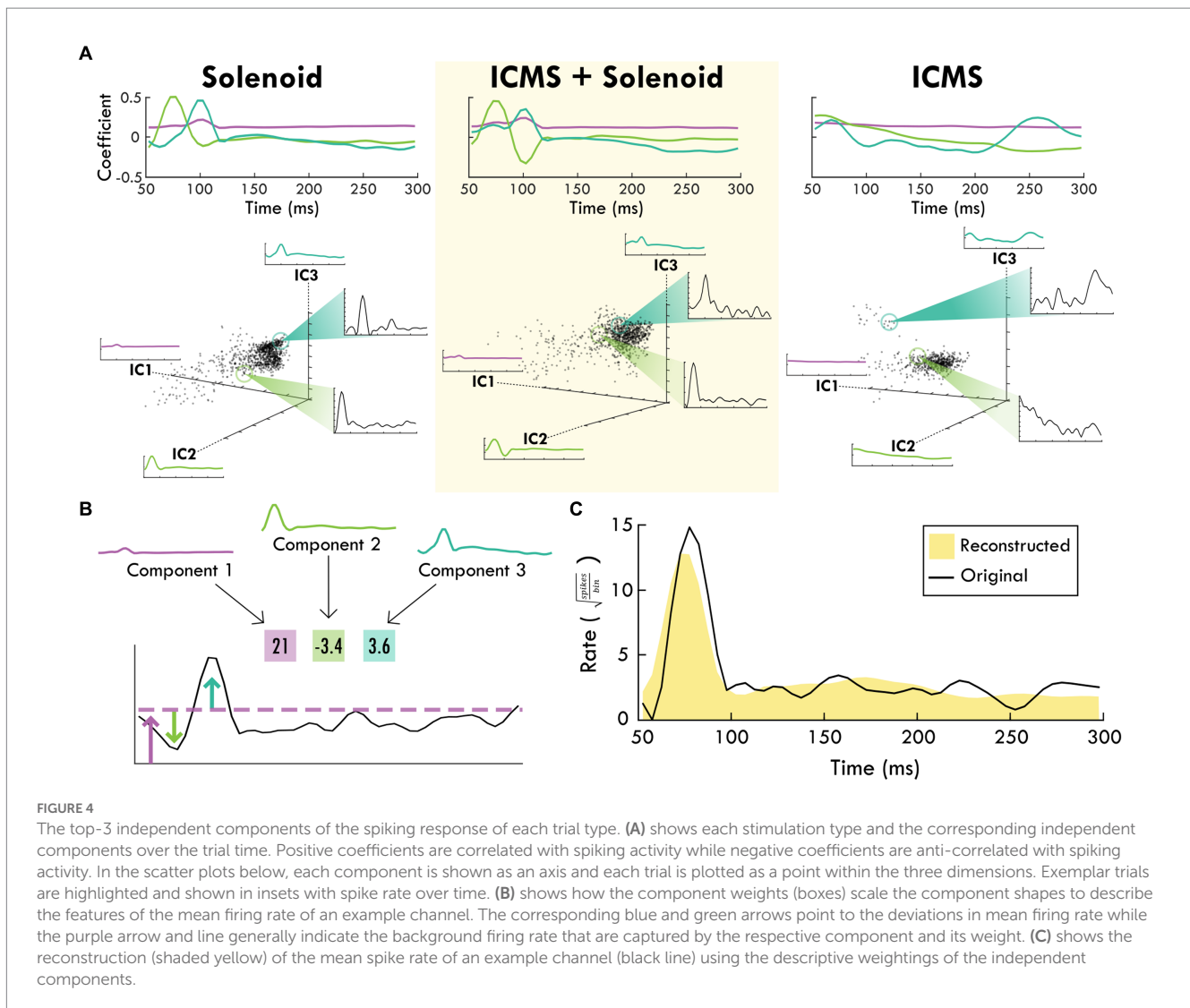
column of x is a different channel's spike rate). In these data, we selected $k=3$, as the top-3 principal components explained most of the observations (Supplementary Figure 5).

2.8. Statistical models

General Linear Mixed Effect models were constructed to test the predictive power of different factors in the weights of the independent components. To fit models, we used the MATLAB (R2020a) 'fitglm' function to fit data with a binomial distribution and logit link function. All models were fit with the 'DummyVarCoding' parameter set to 'effects' (the coefficients must sum to zero), and 'FitMethod' parameter set to 'REML' (restricted maximum pseudo-likelihood estimation for the model optimizer objective function). Two models were created to assess Components 2 and 3 and included terms for the intercept as well as area, lesion volume, trial type, and all their interactions.

3. Results

To investigate the influence of injury on the connection between sensory and premotor cortex, rats had an ischemic lesion induced in the forelimb area of CFA (Figure 1). The lesion was more variable across rats than previously described, with a mean volume of $5.4 \pm 3.7 \text{ mm}^3$ (Supplementary Figure 2; Barbay et al., 2013; Nishibe et al., 2015). The rats were assessed in the skilled reach task to determine severity of motor deficits and recovery profiles. Figure 2A shows the rats' behavioral scores on Days 8, 12, 16 and 20 after the ischemic lesion. As expected, average performance on the reaching task dropped after injury and recovered towards pre-lesion levels by the time the stimulation assays were performed. The majority of the rats had at least one timepoint where their behavioral performance was significantly reduced compared to baseline (4/7 rats had at least one timepoint three standard deviations below baseline, 6/7 rats had one timepoint one standard deviation below; Supplementary Table 1); however, there was a large amount of variance in reaching success overall. Injection of ET-1 was done to target all cortical layers of CFA; however, the resulting lesion had a range of presentations. Categorizing lesions by their anatomical extent explained most of the variance in behavioral performance but did not result in clear patterns in spiking activity (Supplementary Figure 3). An example lesion is shown in Figure 2B. Four weeks after the injury procedure, rats underwent a terminal procedure in which the response to peripheral somatosensory stimulation was recorded in RFA and S1 (Figure 1). Most channels in S1 (92%) had spiking activity which was significantly increased by this stimulation (Supplementary Figure 4). In a subset of trials, ICMS was delivered in RFA alone or preceding the solenoid stimulation to determine if there was modulation of the sensory response. Figure 3 shows the averaged responses of each trial type in both cortical areas. A peak in spiking activity was visible in both RFA and S1 following solenoid-only stimulation. In S1, this response was bimodal with an early increase followed by a second peak 50 ms after solenoid onset; while in RFA, there was a peak which was similar in profile and locked to the same latency as the later peak in S1. With ICMS-only stimulation, there was a peak in spiking activity within RFA



immediately following the pulse that was not observed in S1. In the ICMS + Solenoid condition, there was no obvious modulation in the profiles of the somatosensory-evoked peaks in either area. Most of the averaged responses to any of the trial types did not exceed the threshold of 3 standard deviations above baseline firing with the exception of Solenoid and Solenoid + ICMS responses in RFA which both peaked at 100 ms; however, in all cases the shaded confidence intervals (e.g., Figure 3 inset) surpassed the threshold. This variability suggests that there may be differences in the response at a channel level, leading to the later breakdown of the channel averaged activity by their main features.

The average spiking by trial type was used to identify the principal components of the response to peripheral sensory stimulation from which the independent components were derived. The top independent components help determine underlying trends through dimensionality reduction, explaining a large portion of the data (Supplementary Figures 5, 6). Figure 4B shows an example of the contribution of the top-3 independent components to the somatosensory response with their respective weightings. The top-3 components for each trial type are displayed in Figure 4A starting at

50 ms after the zero point when sensory stimulation begins. The components for the Solenoid and ICMS + Solenoid trials are similar to one another with a relatively flat first component while the next two components have peaks in values at 75 and 100 ms, respectively. The ICMS + Solenoid trials has an additional negative dip in the coefficient of Component 2 at 100 ms that is not seen in the Solenoid-only trials. In comparison, the ICMS trial components have a different pattern than the other trial types. Component 1 is more time invariant whereas Component 2 has a strong positive relationship to the neural data at the trial outset that decreases over the course of the trial to become negative. Component 3 features peaks at 70 and 260 ms; however, between the two peaks the coefficient drops to become negative. Underneath the representation of the independent components, the clustering of the average spike rate for each individual channel in a single experimental block is plotted along the new axes based on their weightings. Overall, the scatterplots highlight patterns in the spiking response along the range of independent features. The insets further capture the descriptive power of the combination of component weightings by displaying the mean spike rate for exemplar points along the component axes. The independent features and their

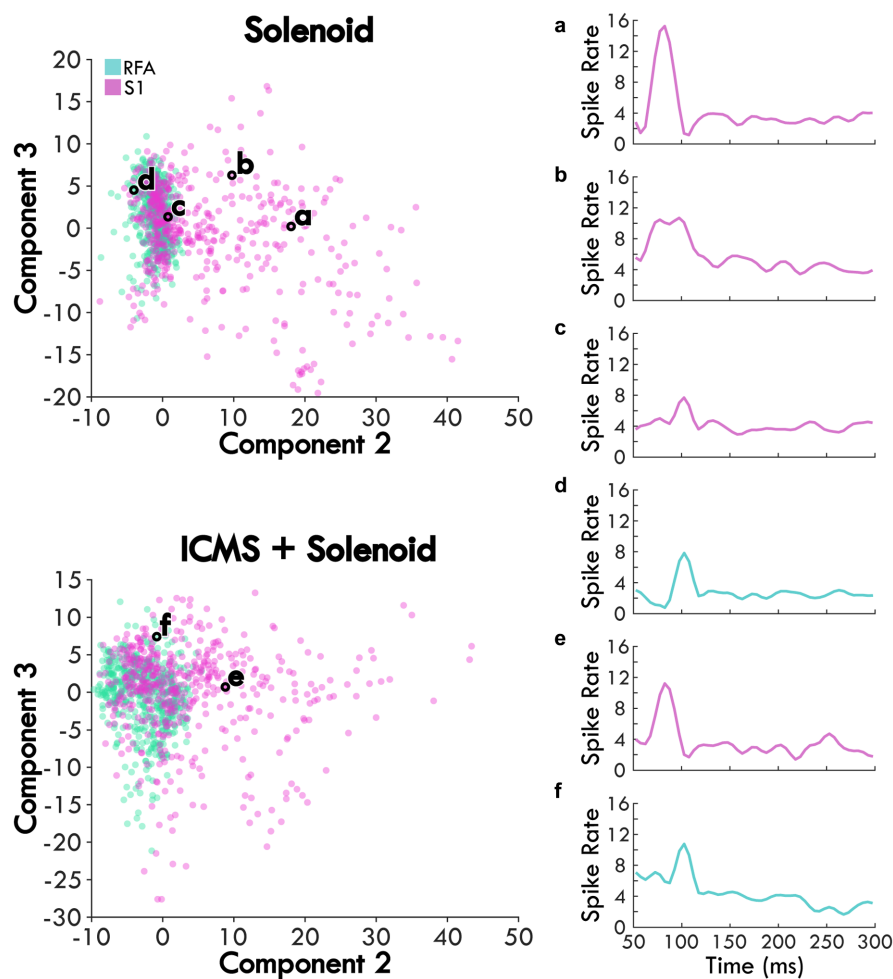


FIGURE 5

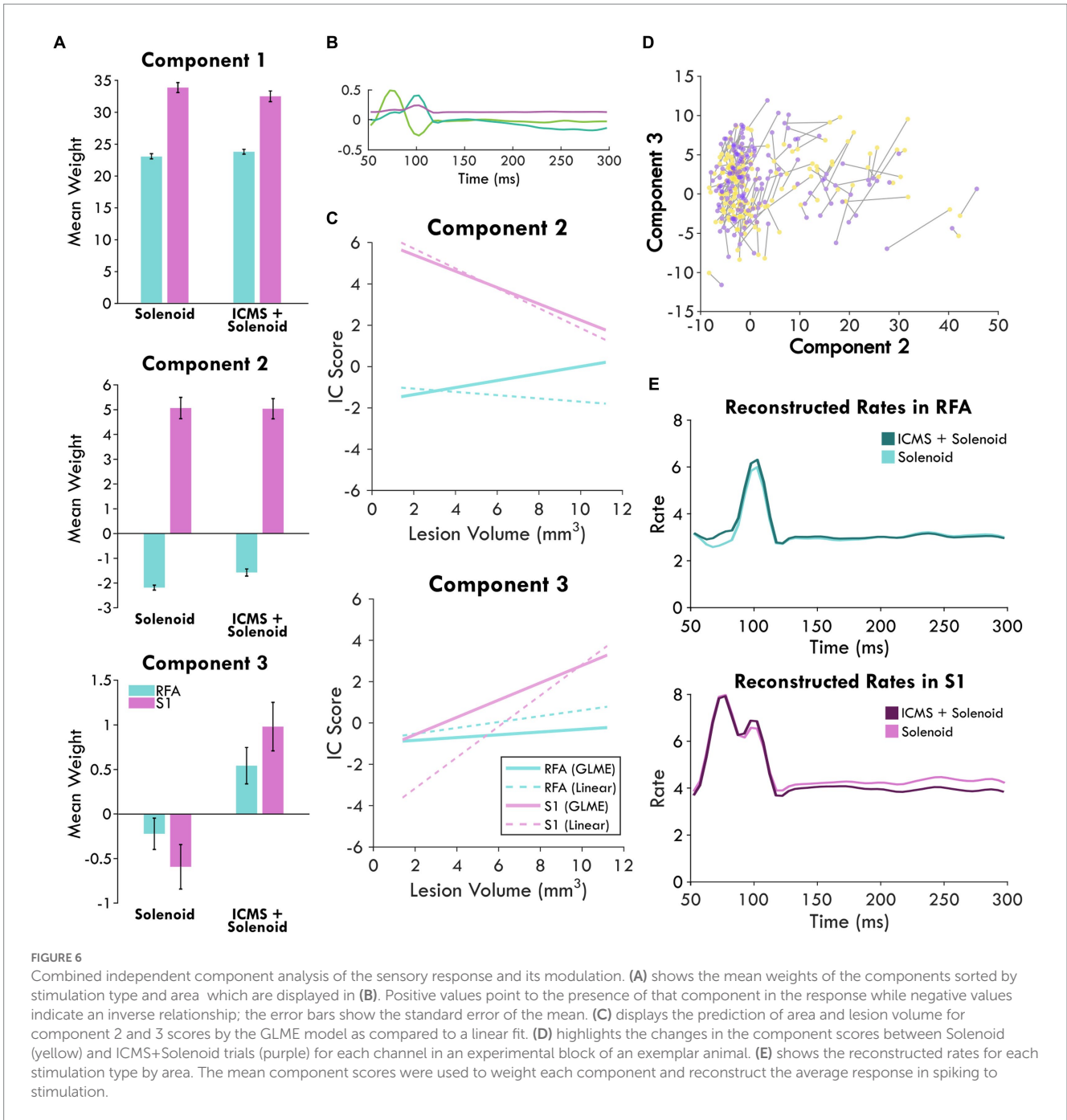
The average scores of Solenoid and ICMS+Solenoid trials in each area. Each channel's spike rate, averaged across an experimental block, is plotted on the second and third component axes based on its score. Channels in RFA are shown as blue and those in S1 are pink. Examples of the average channel spike rates are outlined in black and shown in the subpanels. (a) and (b) two different channels within S1 of the same rat showing different response profiles. (c) channel in S1 of the rat with the largest lesion volume highlighting a smaller first peak. (d) channel in RFA showing a single evoked peak. (e) and (f) the same channels in panels (a) and (d), respectively, during ICMS+Solenoid trials.

respective weightings can be used to reconstruct individual trial rates, capturing the main trends (Figure 4C). For the rest of the analysis, Component 1 was left out as it represents a trial invariant response to stimulation.

Weights for trials were plotted on the axes for Components 2 and 3 to examine trends in the response between Solenoid and ICMS + Solenoid trials by cortical area with breakout panels showing the spike rate of individual trials (Figure 5). The weights along Components 2 and 3 independently capture the early and late portion of the sensory response to represent the peaks in the channel averaged activity (Figures 5A,B). In the Solenoid trials, there is a single cluster for RFA that varies primarily along Component 3. Trials in S1 have a similar cluster with features that resemble that of RFA (Figures 5C,D); however, there is also an additional smear of trials that extend out along the Component 2 axis that have an early increase in spike firing independent of a later peak (Figures 5A,B). With ICMS + Solenoid trials, the patterns of weights shift to be diffusely distributed along both axes (Figure 5). The combined ICMS+Solenoid stimulation

seems to modulate the spike rate in both areas on an individual channel basis, shifting the peaks both positively and negatively (Figures 5E,F).

In order to directly compare the Solenoid and the ICMS + Solenoid response and determine the effect of a leading ICMS pulse, a second set of independent components describing both trial types were derived (Figure 6B). The significance of any difference predicted by experimental variables was quantified using a general linear mixed effects model. The weight of each component was averaged independently for RFA and S1 and found to vary by area and stimulation type (Figure 6A). Area has a significant effect on Component 2—S1 is predicted to produce greater mean values than those in RFA ($RFA = -3.9527 \pm 0.29291$, d.f. = 1946, $p < 0.0001$). Indeed, the mean weight of Component 2 has a positive weight in S1 and a negative weight in RFA in both Solenoid and ICMS + Solenoid trials where the negative weight indicates the inverse component was featured in the data (Figure 6A). Stimulation type is a significant predictor for differences in the mean of



Component 3 and not Component 2 (Component 3: Solenoid = -0.8183 ± 0.17744 , d.f. = 1946, $p < 0.0001$; Component 2: Solenoid = -0.092543 ± 0.25236 , d.f. = 1946, $p = 0.71388$). Component 3 is weakly present on average in both S1 and RFA Solenoid trials; however, with the addition of ICMS in the ICMS + Solenoid trials, the weight of the component increases in both areas (Figure 6A). Additionally, the interaction of area and lesion volume on the mean weight of Component 2 is also significant where larger lesion volumes predict more positive values in RFA and more negative values in S1 (RFA = 0.28152 ± 0.044376 , d.f. = 1946, $p < 0.0001$; Figure 6C). There is no effect of area or lesion volume alone on Component 3; however, area and lesion volume together have a significant interaction (Figure 6C). The mean of the

component is predicted to become more positive in S1 as lesion volume increases whereas in RFA it is relatively unaffected by lesion volume (RFA = -0.17202 ± 0.031232 , d.f. = 1946, $p < 0.0001$). The change in the sensory response with a preceding ICMS pulse is exemplified in Figure 6D where there is a clear shift in the component weights between Solenoid and ICMS + Solenoid trial types. Using the mean component scores for each area, the rates of spiking activity can be reconstructed. Figure 6E shows the modeled rate for Solenoid and ICMS + Solenoid, highlighting the effect of ICMS stimulation on the response in both RFA and S1. The addition of ICMS in the ICMS + Solenoid trials predicts higher spike rates in both cortical areas; there are increased peaks at 100 ms in both and around 75 ms in RFA alone.

4. Discussion

The primary purpose of this study was to probe the connections between somatosensory and premotor cortex after injury to the primary motor cortex by defining the somatosensory-evoked response in the average spike rate and modulating it through the application of a leading ICMS pulse. To assess the modulation of the population spiking rate relative to stimulation, we utilized independent components analysis, using the top three independent components of the data recorded in RFA and S1 for each trial type. These computed independent components were used to reliably describe the response in both areas separately and across stimulation types. Component 1 was time invariant and was related to a general increase in firing and did not provide information relative to stimulation events and was dropped from further analysis while both Components 2 and 3 had clear peaks that were related to increases in spiking activity. We found that there was a response to the solenoid strike in both cortical areas that varied in profile based on lesion volume and stimulation type. The results, along with previous evidence for the importance of CFA to the sensory response in RFA, support the conclusion that there is variable cortical processing of somatosensory responses after damage to CFA (Kunori and Takashima, 2016). This may be a product of underlying anatomical reorganization towards the restitution of sensorimotor integration (Dancause et al., 2005).

4.1. Assessment of the lesion and its impact on cortical sensory responses

Motor information is received in the sensory cortex which can then modulate motor activity (Sanes et al., 1992; Kinnischtzke et al., 2016). The somatosensory-motor network is underpinned by direct corticocortical and corticospinal connections as well as subcortical structures such as corticostriatal and corticothalamic loops (Hooks et al., 2013; Karadimas et al., 2020; Yamawaki et al., 2021). The crosstalk between sensorimotor areas allows for sensory predictions and feedback correction to fine tune the motor output (Kaneko et al., 1994; Ferezou et al., 2007; Mathis et al., 2017). Injury to the motor cortex can result in somatosensory deficits, further exacerbating the observed motor impairments (Nudo et al., 2000). These somatosensory deficits may be mediated by a loss of inhibitory input from primary motor cortex which is important for temporal coding (Fukui et al., 2020). In our study, variable lesion volumes and locations led to heterogeneous behavioral results, but, in general, rats that had larger lesions and greater cortical and subcortical involvement showed increased severity of injury. We expected concurrent modulation of somatosensory information with lesion volume since the corticocortical connections that mediate it were differentially impacted by injury. As a result, we found that lesion volume predicts trends in the spiking response of both cortical areas regardless of stimulation type. The extent of the lesion and the anatomic involvement of neural populations appears to have a significant effect on the sensory response such that any additional modulation by ICMS is obfuscated. Previous work has established the importance of lesion volume and location as predictors for the severity of motor impairment, but the impact on the somatosensory response as well suggests its importance in sensorimotor processing over recovery (Chen et al., 2000).

4.2. Cortical representation of the sensory response after recovery

The premotor cortex is an important site for motor recovery after damage to the primary motor cortex. In addition to extant projections between S1 and the rodent premotor cortex, recovery is often coupled with the formation of *de novo* connections (Dancause et al., 2005; Bedwell et al., 2014). Ischemic injury and the disruption to established connections initiates a cascade of compensatory processes including the upregulation of growth associated genes which can promote dendritic branching and synaptogenesis, supporting functional recovery (Biernaskie et al., 2004; Carmichael et al., 2005). The effects of the molecular response extends beyond the infarct to other cortical areas (Carmichael et al., 2017). While sparse connections exist between RFA and S1, we expect that as premotor cortex takes over function after injury to M1, connectivity to S1 will be strengthened. In uninjured animals, the premotor cortex shows increased activity in response to peripheral somatosensory stimulation; however, the process has been proposed to be mediated by primary motor cortex (Wiesendanger et al., 1985; Kunori and Takashima, 2016). After injury to CFA, there is a clear response to peripheral stimulation in the somatosensory cortex. Interestingly, we also observed a response 50 ms after the solenoid strike in RFA despite the damage to CFA. While we cannot eliminate the potential that with some of the smaller lesions the response was preserved in RFA, the presence of the sensory response in animals even with extensive lesions may indicate the presence of post-ischemic adaptations to restore sensorimotor integration. In S1, where we expect the primary processing of the solenoid stimulus to occur, a similar peak corresponding to 50 ms after sensory stimulation exists in the average solenoid response. However, there is also an earlier peak in activity which is unique to S1, resulting in a bimodal response with peaks at 25 and 50 ms relative to solenoid strike. This early peak in S1 is more likely a traditional somatosensory response associated with somatotopic representation as it aligns with previously cited latencies (Tutunculer et al., 2006) while the later peak 50 ms after solenoid onset may represent some coding of the sensory information with the variation in response profile dependent on the cortical layer and the nearby cell types since its presence on a channel basis is largely variable.

4.3. Evidence for the reorganization of somatosensory processing

Because both RFA and S1 have a similar response which is constrained to the same time point, there must be some factor involved in their synchronicity. The solenoid contact was set to last for 50 ms so the offset would correspond to the later peak in the response; however, the conduction time for a peripheral event such as solenoid offset would have to be nearly instantaneous (Emanuel et al., 2021). Instead, it is more likely that the response is the result of central communication. Neuronal conduction between S1 and RFA was primarily found to be a function of the primary motor cortex under normal conditions and calculated to be on the order of 10 ms, so the longer latency response implies a disruption of normal pathways and subsequent adaptations (Tutunculer et al., 2006; Ferezou et al., 2007; Kunori and Takashima, 2016). Recovery of the somatosensory

response in RFA could alternatively be mediated by thalamocortical projections as the 50 ms latency after solenoid onset does however resemble peak spiking latencies in the thalamus (Sosnik et al., 2001). The synchronous peak might then be explained by this shared input which could be the product of post-injury reorganization. On the other hand, new projections between S1 and RFA as have been shown in previous study may have a longer latency without the mediation of primary motor cortex and could also coordinate the late somatosensory response (Dancause et al., 2005). As a result, the source of the somatosensory evoked peak in spiking within the premotor cortex—whether through direct projections from somatosensory cortex or a shared input—should be further investigated. We propose that anatomical tract tracing studies labeling projections to and from the somatosensory cortex could complement this dataset and provide insight into the source of post-injury plasticity. While the study would be strengthened with a sham lesion group, there were significant predictive effects of lesion volume by area on the component weights which adds evidence that the sensory response is modulated by injury. The effect of lesion volume and area predicts an inverse relationship between Components 2 and 3 of trials in S1 regardless of trial type—with larger lesion volumes the mean weight of Component 2 goes down while Component 3 increases. This could represent a shift from the earlier to the later response particularly as integration of the premotor and somatosensory areas is no longer mediated by the damaged primary motor cortex, instead re-establishing mutual information between the areas after significant disruption. Other work, however, has shown that there is inhibition from primary motor cortex in S1 which is disrupted in injury and the peak increase with larger lesions may alternatively be due to disinhibition (Fukui et al., 2020). In either case, the significance of the later peak of the sensory response is emphasized after injury and, since it is shared by both RFA and S1, supports the plasticity of sensorimotor integration.

4.4. Modulation of the solenoid evoked sensory response

The ICMS pulse was used to probe the connectivity of the two cortical areas by determining if stimulation of RFA influences the somatosensory response of S1 as it does in intact animals (Manita et al., 2015). Analysis of the spiking activity after ICMS-only stimulation highlights a trend for an initial increase in activity which drops with time from the stimulus pulse as represented by Component 2. In RFA where the ICMS stimulation occurred, there was a clear peak in spiking after ICMS delivery. When the ICMS pulse preceded the solenoid stimulation, Component 3, corresponding to the peak 50 ms after the solenoid response, was predicted to have a significantly greater mean weight than solenoid stimulation alone, meaning that on average ICMS facilitated spike firing at this timepoint. Our reconstructed rates further substantiate this by showing that ICMS + Solenoid trials have an elevated peak in RFA. ICMS delivered in RFA shifted the relative firing properties of the neurons within the immediate vicinity of the pulse and likely impacted the processing of somatosensory information. Similarly, the influence of ICMS delivery in RFA on the somatosensory response in S1 predicts an increase in the mean

weight of Component 3 with ICMS + Solenoid stimulation as reflected by the reconstructed rates. We found that there is a clear shift that occurs with the addition of ICMS represented in the distribution of channel-averaged activity along the component axes. Since the representative weights vary with the changes in the underlying rates, the change in the component weights between Solenoid and ICMS + Solenoid trials captures the altered channel averaged activity, including both increased and decreased rates. Based on the current study, it is impossible to ascertain whether ICMS orthodromically activated RFA projections to S1 or if there was antidromic activation of S1 neurons projecting to RFA. Regardless of direction, there is a clear disruption of normal sensory processing in S1 that can be attributed to directly stimulating RFA in ICMS + Solenoid trials. Because there are few direct connections between RFA and S1 and their communication is presumed to be mediated by CFA, the significant influence of stimulation in RFA on activity of S1 despite damage to CFA is interesting and should prompt further study into the source of the effect—whether it be the formation of novel projections as shown in squirrel monkeys after ischemic injury to M1 or the strengthening of existent projections between the areas and where these projections originate (Dancause et al., 2005).

4.5. Inter-channel variability of spiking activity and cortical layer dependence

The independent components may not perfectly fit the mean data but excel at capturing trial to trial variations; therefore, the subtle changes in mean weights and reconstructed rates are only hinting at the diverse population of responses that underly the modulation of sensory processing. This study combined data from different animals, cortical layers, lesion and somatosensory stimulus delivery conditions which contributed to a large amount of heterogeneity in the somatosensory response that was obfuscated by the channel averaged mean. The confidence intervals of the peri-event time histograms had spreads that surpassed the baseline spiking threshold as shown in Figure 3, hinting at the underlying channel variability. Each channel's depth in the cortex depended on the relative depth of the array and the location of the channel on the electrode shank. As a result, the channels measured the relative contribution of neural populations spanning the cortical column; however, projections between sensorimotor cortical areas are layer specific and likely influence the response of local neural populations differently (Mao et al., 2011; Fukui et al., 2020). This study was limited in the ability to discern the location of the electrode site and we chose not to focus on analyzing the averaged response by the cortical layer. However, further studies should examine the contribution of layer-specific somatosensory processing within the cortical column as it could provide insight into participating pathways and cell types.

4.6. Summary

Overall, we found that there was a response in spiking activity in both RFA and S1 even after lesioning of CFA. Part of the

somatosensory response is shared between the two cortical areas and is altered as a function of injury. Component analysis suggests shifts in the response patterns of S1 as a result of stimulation in RFA, implying a functional relationship between RFA and S1 which may be involved in somatosensory processing. Together, these results highlight the response of premotor cortex to peripheral sensory stimulation and the connectivity of sensorimotor cortex after injury, supporting the importance of sensorimotor integration in recovery.

Data availability statement

The raw data supporting the conclusions of this article will be made available by the authors, without undue reservation.

Ethics statement

The animal study was reviewed and approved by Institutional Animal Care and Use Committee at the University of Kansas Medical Center.

Author contributions

MM and DG designed the experiment with input from RN and PH. MM, PH, CT, SD, and JB carried out the experiment. PH and MM analyzed the data. PH interpreted the results, created figures, and wrote up the manuscript with the help of MM. RN and DG edited and guided manuscript development. All authors contributed to the article and approved the submitted version.

References

- Averna, A., Hayley, P., Murphy, M. D., Barban, F., Nguyen, J., Buccelli, S., et al. (2021). Entrainment of network activity by closed-loop microstimulation in healthy ambulatory rats. *Cereb. Cortex* 31, 5042–5055. doi: 10.1093/cercor/bhab140
- Barbay, S., Guggenmos, D. J., Nishibe, M., and Nudo, R. J. (2013). Motor representations in the intact hemisphere of the rat are reduced after repetitive training of the impaired forelimb. *Neurorehabil. Neural Repair* 27, 381–384. doi: 10.1177/1545968312465193
- Bedwell, S. A., Billett, E. E., Crofts, J. J., and Tinsley, C. J. (2014). The topology of connections between rat prefrontal, motor and sensory cortices. *Front. Syst. Neurosci.* 8:00177. doi: 10.3389/fnsys.2014.00177
- Biernaskie, J., Chernenko, G., and Corbett, D. (2004). Efficacy of rehabilitative experience declines with time after focal ischemic brain injury. *J. Neurosci.* 24, 1245–1254. doi: 10.1523/jneurosci.3834-03.2004
- Bundy, D. T., Guggenmos, D. J., Murphy, M. D., and Nudo, R. J. (2019). Chronic stability of single-channel neurophysiological correlates of gross and fine reaching movements in the rat. *PLoS One* 14:e0219034. doi: 10.1371/journal.pone.0219034
- Carè, M., Averna, A., Barban, F., Semprini, M., De Michieli, L., Nudo, R. J., et al. (2022). The impact of closed-loop intracortical stimulation on neural activity in brain-injured, anesthetized animals. *Bioelectron. Med.* 8:4. doi: 10.1186/s42234-022-00086-y
- Carmichael, S. T., Archibeque, I., Luke, L., Nolan, T., Momiy, J., and Li, S. (2005). Growth-associated gene expression after stroke: evidence for a growth-promoting region in peri-infarct cortex. *Exp. Neurol.* 193, 291–311. doi: 10.1016/j.expneurol.2005.01.004
- Carmichael, S. T., and Chesselet, M. F. (2002). Synchronous neuronal activity is a signal for axonal sprouting after cortical lesions in the adult. *J. Neurosci.* 22, 6062–6070. doi: 10.1523/JNEUROSCI.22-14-06062.2002
- Carmichael, S. T., Kathirvelu, B., Schweppe, C. A., and Nie, E. H. (2017). Molecular, cellular and functional events in axonal sprouting after stroke. *Exp. Neurol.* 287, 384–394. doi: 10.1016/j.expneurol.2016.02.007
- Chen, C. L., Tang, F. T., Chen, H. C., Chung, C. Y., and Wong, M. K. (2000). Brain lesion size and location: effects on motor recovery and functional outcome in stroke patients. *Arch. Phys. Med. Rehabil.* 81, 447–452. doi: 10.1053/mr.2000.3837
- Committee for the Update of the Guide for the Care and Use of Laboratory Animals. (2010). *Guide for the Care and Use of Laboratory Animals*. 8th ed. Washington, D.C.: National Academies Press.
- Contestabile, A., Colangiulo, R., Lucchini, M., Gindrat, A. D., Hamadjida, A., Kaeser, M., et al. (2018). Asymmetric and distant effects of a unilateral lesion of the primary motor cortex on the bilateral supplementary motor areas in adult macaque monkeys. *J. Neurosci.* 38, 10644–10656. doi: 10.1523/jneurosci.0904-18.2018
- Dancause, N., Barbary, S., Frost, S. F., Plautz, E. J., Chen, D., Zoubina, E. V., et al. (2005). Extensive cortical rewiring after brain injury. *J. Neurosci.* 25, 10167–10179. doi: 10.1523/jneurosci.3256-05.2005
- Emanuel, A. J., Lehnert, B. P., Panzeri, S., Harvey, C. D., and Ginty, D. D. (2021). Cortical responses to touch reflect subcortical integration of LTMR signals. *Nature* 600, 680–685. doi: 10.1038/s41586-021-04094-x
- Ferezou, I., Haiss, F., Gentet, L. J., Aronoff, R., Weber, B., and Petersen, C. C. H. (2007). Spatiotemporal dynamics of cortical sensorimotor integration in behaving mice. *Neuron* 56, 907–923. doi: 10.1016/j.neuron.2007.10.007
- Foffani, G., Tutunculer, B., and Moxon, K. A. (2004). Role of spike timing in the forelimb somatosensory cortex of the rat. *J. Neurosci.* 24, 7266–7271. doi: 10.1523/jneurosci.2523-04.2004
- Frías, I., Starrs, F., Gisiger, T., Minuk, J., Thiel, A., and Paquette, C. (2018). Interhemispheric connectivity of primary sensory cortex is associated with motor impairment after stroke. *Sci. Rep.* 8:12601. doi: 10.1038/s41598-018-29751-6
- Friel, K. M., Barbay, S., Frost, S. B., Plautz, E. J., Hutchinson, D. M., Stowe, A. M., et al. (2005). Dissociation of sensorimotor deficits after rostral versus caudal lesions in the primary motor cortex hand representation. *J. Neurophysiol.* 94, 1312–1324. doi: 10.1152/jn.01251.2004

Funding

This work was supported by NIH Grant R01NS030853 and NIH Grant T32HD057850-11A1.

Acknowledgments

Thanks to Jasmine Deng for her surgical assistance.

Conflict of interest

The authors declare that the research was conducted in the absence of any commercial or financial relationships that could be construed as a potential conflict of interest.

Publisher's note

All claims expressed in this article are solely those of the authors and do not necessarily represent those of their affiliated organizations, or those of the publisher, the editors and the reviewers. Any product that may be evaluated in this article, or claim that may be made by its manufacturer, is not guaranteed or endorsed by the publisher.

Supplementary material

The Supplementary material for this article can be found online at: <https://www.frontiersin.org/articles/10.3389/fnins.2023.1151309/full#supplementary-material>

- Fukui, A., Osaki, H., Ueta, Y., Kobayashi, K., Muragaki, Y., Kawamata, T., et al. (2020). Layer-specific sensory processing impairment in the primary somatosensory cortex after motor cortex infarction. *Sci. Rep.* 10:3771. doi: 10.1038/s41598-020-60662-7
- Harrison, T. C., Silasi, G., Boyd, J. D., and Murphy, T. H. (2013). Displacement of sensory maps and disorganization of motor cortex after targeted stroke in mice. *Stroke* 44, 2300–2306. doi: 10.1161/strokeaha.113.001272
- Hooks, B. M., Mao, T., Gutnisky, D. A., Yamawaki, N., Svoboda, K., and Shepherd, G. M. G. (2013). Organization of Cortical and Thalamic Input to pyramidal neurons in mouse motor cortex. *J. Neurosci.* 33, 748–760. doi: 10.1523/jneurosci.4338-12.2013
- Kaneko, T., Caria, M. A., and Asanuma, H. (1994). Information processing within the motor cortex. II. Intracortical connections between neurons receiving somatosensory cortical input and motor output neurons of the cortex. *J. Comp. Neurol.* 345, 172–184. doi: 10.1002/cne.903450203
- Karadimas, S. K., Satkunendrarajah, K., Laliberte, A. M., Ringuette, D., Weisspapir, I., Li, L., et al. (2020). Sensory cortical control of movement. *Nat. Neurosci.* 23, 75–84. doi: 10.1038/s41593-019-0536-7
- Kim, Y., Kim, W. S., Koh, K., Yoon, B., Damiano, D. L., and Shim, J. K. (2016). Deficits in motor abilities for multi-finger force control in hemiparetic stroke survivors. *Exp. Brain Res.* 234, 2391–2402. doi: 10.1007/s00221-016-4644-2
- Kinnischtzke, A. K., Fanselow, E. E., and Simons, D. J. (2016). Target-specific M1 inputs to infragranular S1 pyramidal neurons. *J. Neurophysiol.* 116, 1261–1274. doi: 10.1152/jn.01032.2015
- Kunori, N., and Takashima, I. (2016). High-order motor cortex in rats receives somatosensory inputs from the primary motor cortex via cortico-cortical pathways. *Eur. J. Neurosci.* 44, 2925–2934. doi: 10.1111/ejn.13427
- Lee, M. C., Kim, R. G., Lee, T., Kim, J. H., Lee, K. H., Choi, Y. D., et al. (2020). Ultrastructural dendritic changes underlying Diaschisis after capsular infarct. *J. Neuropathol. Exp. Neurol.* 79, 508–517. doi: 10.1093/jnen/nlaa001
- Manita, S., Suzuki, T., Homma, C., Matsumoto, T., Odagawa, M., Yamada, K., et al. (2015). A top-down cortical circuit for accurate sensory perception. *Neuron* 86, 1304–1316. doi: 10.1016/j.neuron.2015.05.006
- Mao, T., Kusefoglu, D., Hooks, B. M., Huber, D., Petreanu, L., and Svoboda, K. (2011). Long-range neuronal circuits underlying the interaction between sensory and motor cortex. *Neuron* 72, 111–123. doi: 10.1016/j.neuron.2011.07.029
- Mathis, M. W., Mathis, A., and Uchida, N. (2017). Somatosensory cortex plays an essential role in forelimb motor adaptation in mice. *Neuron* 93, 1493–1503.e6. doi: 10.1016/j.neuron.2017.02.049
- Moxon, K. A., Hale, L. L., Aguilar, J., and Foffani, G. (2008). Responses of infragranular neurons in the rat primary somatosensory cortex to forepaw and hindpaw tactile stimuli. *Neuroscience* 156, 1083–1092. doi: 10.1016/j.neuroscience.2008.08.009
- Mukhopadhyay, S., and Ray, G. C. (1998). A new interpretation of nonlinear energy operator and its efficacy in spike detection. *IEEE Trans. Biomed. Eng.* 45, 180–187. doi: 10.1109/10.661266
- Nasir, S. M., Darainy, M., and Ostry, D. J. (2013). Sensorimotor adaptation changes the neural coding of somatosensory stimuli. *J. Neurophysiol.* 109, 2077–2085. doi: 10.1152/jn.00719.2012
- Nishibe, M., Barbay, S., Guggenmos, D., and Nudo, R. J. (2010). Reorganization of motor cortex after controlled cortical impact in rats and implications for functional recovery. *J. Neurotrauma* 27, 2221–2232. doi: 10.1089/neu.2010.1456
- Nishibe, M., Urban, E. T. R., Barbay, S., and Nudo, R. J. (2015). Rehabilitative training promotes rapid motor recovery but delayed motor map reorganization in a rat cortical ischemic infarct model. *Neurorehabil. Neural Repair* 29, 472–482. doi: 10.1177/1545968314543499
- Nudo, R. J., Friel, K. M., and Delia, S. W. (2000). Role of sensory deficits in motor impairments after injury to primary motor cortex. *Neuropharmacology* 39, 733–742. doi: 10.1016/s0028-3908(99)00254-3
- Padberg, J., Recanzone, G., Engle, J., Cooke, D., Goldring, A., and Krubitzer, L. (2010). Lesions in posterior parietal area 5 in monkeys result in rapid behavioral and cortical plasticity. *J. Neurosci.* 30, 12918–12935. doi: 10.1523/JNEUROSCI.1806-10.2010
- Paxinos, G., and Watson, C. (2006). *The Rat Brain in Stereotaxic Coordinates*. Amsterdam: Academic Press/Elsevier.
- Rouiller, E. M., Moret, V., and Liang, F. (1993). Comparison of the connective properties of the two forelimb areas of the rat sensorimotor cortex: support for the presence of a premotor or supplementary motor cortical area. *Somatosens. Mot. Res.* 10, 269–289. doi: 10.1016/08990229309028837
- Sanes, J. N., Wang, J., and Donoghue, J. P. (1992). Immediate and delayed changes of rat motor cortical output representation with new forelimb configurations. *Cereb. Cortex* 2, 141–152. doi: 10.1093/cercor/2.2.141
- Shadmehr, R., and Krakauer, J. W. (2008). A computational neuroanatomy for motor control. *Exp. Brain Res.* 185, 359–381. doi: 10.1007/s00221-008-1280-5
- Shadmehr, R., Smith, M. A., and Krakauer, J. W. (2010). Error correction, sensory prediction, and adaptation in motor control. *Annu. Rev. Neurosci.* 33, 89–108. doi: 10.1146/annurev-neuro-060909-153135
- Sosnik, R., Haidarliu, S., and Ahissar, E. (2001). Temporal frequency of whisker movement. I. Representations in brain stem and thalamus. *J. Neurophysiol.* 86, 339–353. doi: 10.1152/jn.2001.86.1.339
- Sweetnam, D. A., and Brown, C. E. (2013). Stroke induces long-lasting deficits in the temporal fidelity of sensory processing in the somatosensory cortex. *J. Cereb. Blood Flow Metab.* 33, 91–96. doi: 10.1038/jcbfm.2012.135
- Thoroughman, K. A., and Shadmehr, R. (2000). Learning of action through adaptive combination of motor primitives. *Nature* 407, 742–747. doi: 10.1038/35037588
- Tseng, Y., Diedrichsen, J., Krakauer, J. W., Shadmehr, R., and Bastian, A. J. (2007). Sensory prediction errors drive cerebellum-dependent adaptation of reaching. *J. Neurophysiol.* 98, 54–62. doi: 10.1152/jn.00266.2007
- Tutunculer, B., Foffani, G., Himes, B. T., and Moxon, K. A. (2006). Structure of the excitatory receptive fields of Infragranular forelimb neurons in the rat primary somatosensory cortex responding to touch. *Cereb. Cortex* 16, 791–810. doi: 10.1093/cercor/bhj023
- Vidoni, E. D., Acerra, N. E., Dao, E., Meehan, S. K., and Boyd, L. A. (2010). Role of the primary somatosensory cortex in motor learning: an rTMS study. *Neurobiol. Learn. Mem.* 93, 532–539. doi: 10.1016/j.nlm.2010.01.011
- Wiesendanger, M., Hummelsheim, H., and Bianchetti, M. (1985). Sensory input to the motor fields of the agranular frontal cortex: a comparison of the precentral, supplementary motor and premotor cortex. *Behav. Brain Res.* 18, 89–94. doi: 10.1016/0166-4328(85)90065-8
- Yamawaki, N., Raineri Tapies, M. G., Stults, A., Smith, G. A., and Shepherd, G. M. (2021). Circuit organization of the excitatory sensorimotor loop through hand/forelimb S1 and M1. *elife* 10:e66836. doi: 10.7554/eLife.66836